



## Tradeoffs Between Irradiance Capture and Avoidance in Semi-arid Environments Assessed with a Crown Architecture Model

FERNANDO VALLADARES† and FRANCISCO I. PUGNAIRE‡

\* Centro de Ciencias Medioambientales, C.S.I.C. Serrano 115 dpdo, 28006 Madrid, Spain and ‡ Estación Experimental de Zonas Áridas, C.S.I.C. General Segura 1, 04001 Almería, Spain

Received: 24 August 1998 Returned for revision: 10 November 1998 Accepted: 2 January 1999

Plants in arid environments cope with stress from excessive irradiance by physiological photoprotection of the photosynthetic apparatus and by structurally reducing the leaf area exposed to the sun (structural photoprotection). We assessed the ecological relevance of structural photoprotection in two plants of contrasting architecture co-occurring in a semi-arid environment, using the three-dimensional canopy model YPLANT. We compared the role of crown geometry in avoiding excessive radiation, analysed the costs of structural photoprotection in terms of reduction of potential carbon gain, and compared these costs with those due to seasonal constraints of photosynthesis and tissue ageing. The results of the model simulations indicated that canopy architecture of *Stipa tenacissima* (a tussock grass) and *Retama sphaerocarpa* (a leafless leguminous shrub) minimized the risk of overheating and photo-oxidative destruction of the photosynthetic apparatus with steeply oriented foliage and moderate self-shading. But this structural photoprotection imposed an increased cost in terms of potential carbon gain. Diurnal and seasonal patterns of light interception by the crown of these plants translated into a simulated potential carbon gain only half that of an equivalent, horizontal photosynthetic surface. This reduction in potential carbon gain, due to irradiance avoidance, was similar to that imposed by water shortage. *S. tenacissima*, which ceases photosynthetic activity during periods of drought, exhibited more structural avoidance of irradiance than *R. sphaerocarpa*, which remains active throughout the year. This illustrates the influence of the capacity of plants to utilize light for carbon fixation on the trade-offs between irradiance capture and avoidance. Structural avoidance of excessive radiation efficiently prevents the risk of damage by intense irradiance, has no special maintenance costs, and is biomechanically cheaper than enhanced light harvesting by a horizontal canopy, which points to structural photoprotection as a very effective strategy to cope with high irradiance stress in poor and adverse habitats.

© 1999 Annals of Botany Company

**Key words:** Canopy model, functional architecture, irradiance avoidance, light harvesting, photoinhibition, photoprotection, photosynthesis model, plant architecture, *Retama sphaerocarpa*, semi-arid environment, *Stipa tenacissima*, structural photoprotection.

### INTRODUCTION

Excess light decreases the efficiency of photosynthesis, and most plants experience some degree of photoinhibition especially in adverse environments such as arid zones and at high latitudes and elevations (Powles, 1984; Long, Humphries and Falkowski, 1994; Horton, Ruban and Walters, 1996). High light interception may also lead to overheating of the leaf especially when transpirational leaf cooling is restrained by water deficit (Gamon and Pearcy, 1989, 1990; Larcher, 1995; Valladares and Pearcy, 1997). In these environments plants follow two strategies, which are not mutually exclusive. One is physiological photoprotection of the photosynthetic apparatus when light intensities are in excess of those that can be utilized in photosynthesis. Many studies have been devoted to this strategy in the last two decades, and have shown a remarkable capacity of down-regulation and non-photochemical dissipation of excitation energy of the photosynthetic apparatus (Demmig-Adams and Adams, 1992; Anderson, Chow and Öquist, 1993;

Long *et al.*, 1994; Horton *et al.*, 1996). The other strategy is structural avoidance of excessive irradiance (structural photoprotection), which plants achieve by reducing the leaf area directly exposed to the sun. Quantitative information on the fraction of the irradiance avoided by the foliage of wild plants in xeric environments has seldom been reported although the importance of structural attributes, such as leaf angle, in plant photoprotection has been noted frequently (McMillen and McClendon, 1979; Werk and Ehleringer, 1984; Smith and Ullberg, 1989; Ryel, Beyschlag and Caldwell, 1993; Ryel and Beyschlag, 1995; Valladares and Pearcy, 1997, 1998).

Structural avoidance of excessive irradiance can be achieved either by a dense crown (high self-shading and poor light penetration to the lower layers of the foliage), by steep photosynthetic surfaces, or by a combination of the above, as is the general situation in nature (Herbert, 1996; Valladares and Pearcy, 1998). However, dense crowns are usually made up of a steeply inclined foliage in order to reach a balance between photoprotection and carbon gain. Because of the complexity of the light environment within a plant canopy, analysis of light interception by photosynthetic surfaces and the corresponding potential carbon

† For correspondence. Fax 34 91 5640800, e-mail valladares@ccma.csic.es

gain is best accomplished via computer models, and a rather large number of photosynthesis models have been used for this purpose. These models can be grouped in two categories: (1) deterministic, geometrically-based models which use ray tracing techniques (e.g. Niklas, 1988; Dickmann *et al.*, 1990; Takenaka, 1994); and (2) statistical models in which the probability of light penetration to a particular canopy layer is calculated (e.g. Caldwell *et al.*, 1986; Ryel *et al.*, 1993).

In this study we assess the ecological relevance of structural photoprotection using the three-dimensional, geometrically-based canopy model YPLANT (Percy and Yang, 1996) for calculations of whole plant light interception and carbon gain in two different species co-occurring in a semi-arid environment. This model has been recently applied to explore the role of sun and shade plant architectures in light interception and photosynthesis in a sclerophyll chaparral shrub (Valladares and Percy, 1998). The model was applied to two species of contrasting morphology from semi-arid environments in SE Spain: a tussock grass, *Stipa tenacissima*, and a leafless leguminous shrub, *Retama sphaerocarpa*. While *R. sphaerocarpa* has a deep root system (Haase *et al.*, 1996) which makes photosynthetic activity possible throughout the whole year, *S. tenacissima* has shallow roots and activity ceases during drought (Pugnaire *et al.*, 1996a). We hypothesized that *S. tenacissima* would exhibit larger photoprotection due to its shorter period of photosynthetic activity, so the exposure of green tissues could be reduced during non-productive periods under potentially harmful high light and temperature conditions. Our objectives were to compare the influence of different canopy geometries in avoidance of excessive light and to analyse the costs of structural photoprotection in terms of potential carbon gain. Finally, we compared these costs with those due to seasonal constraints of photosynthesis (mostly water deficit) and tissue ageing.

## MATERIALS AND METHODS

### *Field site and species*

The field site was located in Rambla Honda, a valley in the southern foothills of the Sierra de Los Filabres range near Tabernas, Almería Province, Spain (37°08' N, 2°22' W, 630 m elevation). The climate in the region is semi-arid, with a mean annual precipitation of 242 mm, and a pronounced dry season from June to September in which there is no rain in most years (for more information see Pugnaire and Haase, 1995; Pugnaire *et al.*, 1996a, b). The lack of clouds together with the latitude translates into high radiation loads. The site experiences direct sun (radiation > 120 W m<sup>-2</sup>) for 72–85% of the day, averaged over a year (Table 1). Mean total radiation is 19–34 MW m<sup>-2</sup> d<sup>-1</sup>, of which approx. one-fifth is received as diffuse sky radiation (Table 1). The region supports plant communities in which scattered leguminous shrubs such as the summer deciduous *Anthyllis cytisioides* L. and the evergreen *Retama sphaerocarpa* (L.) Boiss. often mixed with the perennial grass *Stipa tenacissima* L., predominate. In some areas there are steppe-like habitats dominated by *S. tenacissima*, a long-living

perennial grass that forms tussocks and spreads vegetatively. It has long, narrow, cylindrical leaves arranged in tillers, with each individual tiller usually having several senescent or dead leaves and two to three green leaves (Sánchez and Puigdefábregas, 1994; Sánchez, 1995). Growth rate of this species is extremely slow. Root:shoot ratio in *S. tenacissima* is very small and the plant arrests growth during the summer, when water deficit reaches a maximum. However, the arrested development of *S. tenacissima* leaves is not due to summer dormancy because leaves respond opportunistically within days to pulses of water (Pugnaire *et al.*, 1996a). *R. sphaerocarpa* is a practically leafless, N-fixing shrub with cylindrical photosynthetic stems, called cladodes. The cladodes are produced annually, and at any one time there may be two to three cohorts present. The new cladodes grow from the axillary buds of the previous year's cohort so that the shrub becomes multi-stemmed, with a large number of branches of different lengths. The largest shrubs of *R. sphaerocarpa* may reach more than 4 m in height, but most are between 2 and 3 m tall. The deep root system of *R. sphaerocarpa* may draw water from a depth of 20–30 m (Haase *et al.*, 1996), allowing the shrub to maintain physiological activity throughout the year.

### *Three-dimensional reconstruction of crown architecture*

The three-dimensional computer model YPLANT created by Percy and Yang (1996) was used to simulate above-ground architecture of the two species and to calculate the light interception and carbon gain for the whole canopy. The model constructs the plant node by node, creating a leaf as a three-dimensional vector space with a given azimuth, angle from the horizontal, and distance to the next node. The vector for petioles was determined in a similar way. Leaves were connected at the distal end of the petiole with their position in space determined by the angle and azimuth of the normal to the surface, the azimuth of the longitudinal axis corresponding to the midrib. Measurements of azimuths and angles were made with a compass and an angle finder constructed from a level and protractor, respectively. Full details of the measurement procedure and the model are given in Percy and Yang (1996), and additional information and examples can be found in Valladares and Percy (1998) and Percy and Yang (1998). The measurements were then used in YPLANT to reconstruct a three dimensional image of the plant canopy. By rotating this image to specific vectors corresponding to a direction of incident photosynthetic photon flux density (PPFD), YPLANT calculated the fraction of PPFD from this direction that would be intercepted. Simulations of direct PPFD interception were based on the interception of light from the angle and azimuth of the solar disc at specified intervals over the day. Simulations of diffuse PPFD absorption were based on vectors for 160 different sky sectors (eight azimuth and 20 zenith angle classes). Calculations of PPFD interception by YPLANT either in the open or in the understorey have been shown to accurately match PPFD values measured with light sensors mounted on the surface of the leaves of the plants (Percy and Yang, 1996; Valladares and Percy, 1998).

TABLE 1. Mean day length, number of hours of sun, total daily radiation and diffuse radiation in Tabernas (Almería, Spain) for the period 1993–98

Season	Day length (h)	Hours of sun* (fraction of day length)	Total radiation† (MW m <sup>-2</sup> d <sup>-1</sup> )	Diffuse radiation (fraction of total)
Winter	9.7 (0.04)	0.72 (0.20)	18.9 (0.26)	0.17 (0.30)
Spring	12.4 (0.10)	0.79 (0.05)	27.9 (0.14)	0.20 (0.03)
Summer	14.3 (0.02)	0.85 (0.06)	34.2 (0.02)	0.19 (0.07)
Autumn	11.5 (0.10)	0.67 (0.11)	21.3 (0.24)	0.21 (0.03)

Data are means for each season plus the coefficient of variation in parentheses.

\* Expressed as a fraction of day length with direct radiation > 120 W m<sup>-2</sup>.

† An estimate of daily PPFD in mol m<sup>-2</sup> can be obtained by multiplying each value by 1.812, the ratio of solar constants.

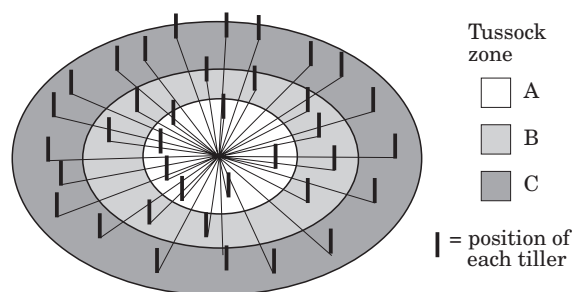


FIG. 1. Arrangement of the horizontal stems (radial lines) and the base of *Stipa tenacissima* tillers (vertical lines) used in the reconstruction of the plant with the 3-D computer model. The tillers were distributed in three concentric zones in direct proportion to the surface area of each zone. The radius of the external ring was 11.3 cm.

Quantification of the relative performance of the canopy architecture was made on the basis of several different measures of efficiency. The projected leaf area normal to incident PPFD is the actual leaf area reduced by the cosine of incidence, and the projection efficiency ( $E_p$ ) is the ratio of the potential projected leaf area to the actual leaf area. It expresses the angular effects on light interception in the absence of leaf overlap (self-shading) in this direction. The displayed area is the projected area as reduced by leaf overlap. The display efficiency ( $E_D$ ) is the ratio of the displayed area to the actual leaf area.

Data for the reconstruction of a tussock of *S. tenacissima* with YPLANT were obtained in the field and were completed with the available quantitative information regarding the modular nature of this plant (Sánchez and Puigdefábregas, 1994; Sánchez, 1995). The basic unit of the tussocks of *S. tenacissima* are the stems. The apical end of the stem is formed by a tiller, which includes the growing axis with its leaves. The leaves are up to 1 m long, and after dying they bend down and may persist for years forming a rigid, interwoven mat. The reconstructed plant of *S. tenacissima* had 40 tillers placed at the end of 40 horizontal stems of varying lengths radiating from the centre of the tussock (Fig. 1). The longest horizontal stem was 11.3 cm and was taken as the radius of the base of the tussock. This radius was divided in three segments to distinguish three concentric rings (zones A, B, and C; Fig. 1). The azimuth and length of each stem were taken at random, provided

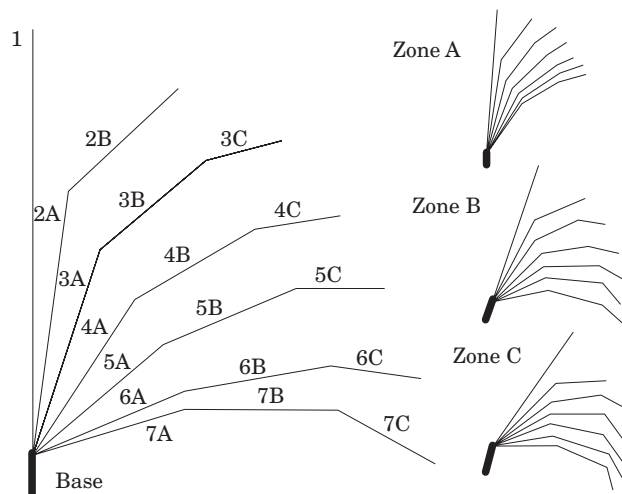


FIG. 2. Diagram of a *Stipa tenacissima* tiller showing the seven leaves attached to a small base, and the several segments considered in leaves 2–7 in order to mimic the curvature of long leaves. Lengths and angles of leaf segments were different for the three different zones of the tussock (A, B, C), as illustrated on the right hand side (see Table 2 for the actual values entered in the 3-D computer model).

that the number of tillers placed in each zone was proportional to the surface area of the zone. Each tiller had a small base (equivalent to the dry base of the real tillers made up by old sheaths), which had the same orientation as the horizontal stem to which it was attached (Fig. 1). The mean elevation angle and length of this small base varied with the zone: 90° and 16 cm in zone A, 75° and 11 cm in zone B, and 65° and 6 cm in zone C. Each tiller had, on average, three green and four dry leaves (Fig. 2). With the exception of leaf 1, all leaves were divided in two–three segments to mimic the curvature of real leaves. Elevation angles and lengths of the different segments of each leaf varied with the zone of the tussock (values shown in Table 2). Angles of leaf 1 were taken at random between the limits shown in Table 2. The azimuth of each leaf segment was the same as the stem, except for the last segment of the leaves 3 to 7, which had a random azimuth between that of the stem  $\pm 90^\circ$ . The resulting plant was 0.7 m in height and had a photosynthetic surface of 2101 cm<sup>2</sup>, with an additional 2038 cm<sup>2</sup> of senesced foliage (Fig. 3). To simulate light

TABLE 2. Angles and lengths of the different segments of leaves of *Stipa tenacissima* entered into the crown architecture model

Segment	Angle			Length (cm)		
	Zone A	Zone B	Zone C	Zone A	Zone B	Zone C
1	80–90	68–78	55–67	35	28	26
2a	85	70	60	40	37	34
2b	60	55	50	20	18	16
3a	80	65	55	38	37	36
3b	55	25	0	10	8	6
3c	30	–40	–55	12	10	8
4a	70	55	40	34	33	32
4b	35	20	5	14	12	10
4c	0	15	–30	12	10	8
5a	60	45	30	30	29	28
5b	25	10	–5	18	16	14
5c	–10	–25	–40	12	10	8
6a	50	35	20	15	15	24
6b	12	12	–12	15	14	8
6c	–20	–35	–50	18	16	8
7a	40	25	10	10	10	19
7b	12	–12	–27	20	19	10
7c	–30	–45	–60	18	16	9

The plant was divided into three concentric rings (zones A, B and C; Fig. 1) and each tiller had seven leaves articulated in one–three segments (leaves 1 to 7, segments a, b and c; Fig. 2) to mimic the curvature of the leaves. Data are mean values obtained from field measurements combined with information in Sánchez (1995) and Sánchez and Puigdefábregas (1994).

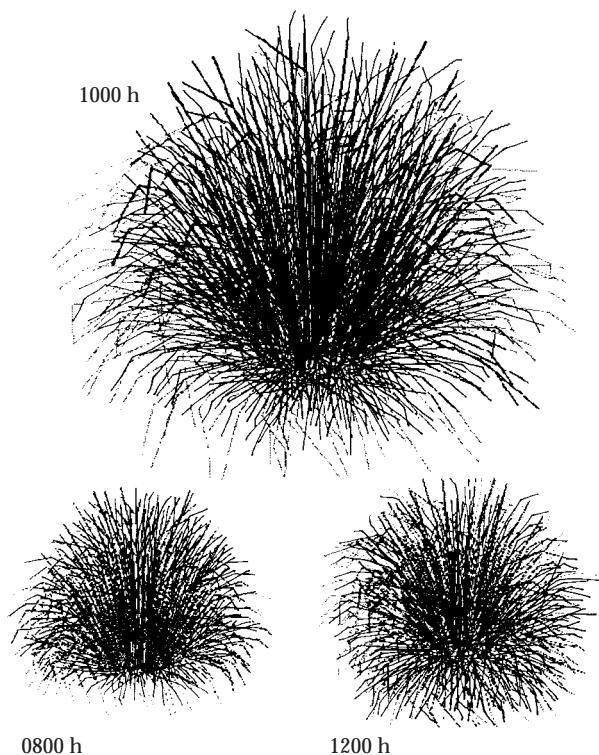


FIG. 3. Computer images of a reconstructed *Stipa tenacissima* tussock as viewed from the sunpath at different times of the day in spring (April 1). The plant is 0.7 m high.



FIG. 4. Computer images of a reconstructed *Retama sphaerocarpa* shrub as viewed from the sunpath at different times of the day in spring (April 1). The plant is 1.5 m high.

interception by photosynthetically active tissues in plants with different proportions of green and senesced surfaces, each leaf segment was converted into dry or senesced units following the observed patterns of leaf senescence. The order of transformation of green leaf segments into senesced ones was 3C-3B-3A-2B-2A. The order followed to reduce the amount of attached senesced leaves was 7-6-5-4.

We obtained the geometric information required to reconstruct the crown of *R. sphaerocarpa* on plants in the field. Elevation angle, length, diameter and orientation of each cladode and stem was determined for three different branches. The resulting plant was 1.5 m in height and had a photosynthetic surface of 1114.5 cm<sup>2</sup> (Fig. 4).

YPLANT 3-D reconstruction of the crown architecture was checked for the two study species. The shadow area of a small shoot was compared to that predicted by YPLANT. One shoot of each species was cut off and its shadow projected onto a piece of white paper used as a rear projection screen once the structural measurements required by YPLANT were taken. A picture was taken from the rear to get an image of the shadow. The paper was always kept normal to the source of light but the angle and azimuth of the shoot was varied. The problem with this sort of validation is penumbral effects (not considered in YPLANT), especially when the structures are small in diameter and far from the paper. Despite this source of error, the differences between simulated projected areas by

TABLE 3. Maximum rates of net photosynthesis of leaves of *Stipa tenacissima* and cladodes of *Retama sphaerocarpa* of different ages and in different months used in model calculations

	January	April	July	September
<i>Stipa tenacissima</i>				
Current year (young)	11 (0.08)	13 (0.09)	2 (0.10)	1.5 (0.08)
1–1.5 years old (mature)	11 (0.07)	16 (0.10)	2 (0.08)	1.5 (0.11)
> 1.5 years old (old)	5 (0.10)	5.5 (0.09)	2 (0.07)	1.5 (0.11)
<i>Retama sphaerocarpa</i>				
Current year (young)	20 (0.11)	13 (0.09)	10 (0.08)	25 (0.11)
1–2 years old (mature)	20 (0.11)	15 (0.09)	7 (0.12)	20 (0.08)
> 2 years old (old)	18 (0.09)	13 (0.08)	7 (0.11)	18 (0.11)

Data are mean values plus coefficient of variation (in parentheses) obtained in different studies carried out in the same location (see Pugnaire *et al.*, 1996a and b; Haase *et al.*, 1999a, b).

YPLANT and measured areas projected in the rear projection screen were  $5 \pm 2\%$  for ten different perspectives of each shoot. This result provided further support to the accuracy of YPLANT in modelling a 3-D crown for simulations of light interception.

#### Estimations of carbon gain by the whole crown

The computer model calculated carbon gain by combining the estimated light interception by the plant canopy with values of net photosynthesis, dark respiration and photosynthetic quantum yield from light response curves measured in the field. Gas exchange, water status and the extent of photoinhibition throughout different seasons of the year were measured on different days and under different environmental conditions during the period 1992–1995 for *S. tenacissima* leaves and *R. sphaerocarpa* cladodes (Pugnaire and Haase, 1995; Pugnaire *et al.*, 1996a and b; Haase *et al.*, 1999a). The maximum rates of net carbon uptake ( $A_{\max}$  on a surface area basis) were much higher in *R. sphaerocarpa* than in *S. tenacissima*. Dark respiration was around 5% of the corresponding  $A_{\max}$  for a given season and age, except in the case of the cladodes of *R. sphaerocarpa* during the period of active growth (April), when it was 10% of  $A_{\max}$ . The PPFD at which 90% of  $A_{\max}$  was reached by an average photosynthetic surface of either species was  $1600 \mu\text{mol m}^{-2} \text{s}^{-1}$ . PPFD above saturation in the text refers to values above this. Potential carbon gain of the two canopies was simulated for January 1, April 1, July 1 and September 30 considering the effects of seasonal constraints on photosynthesis. Carbon gain by the whole crown is compared in the text and in some graphs with that by an equivalent, horizontal photosynthetic surface with no self-shading and with the same photosynthetic response to light as the plant in question.

The photosynthetic tissues were classified into three age classes after Haase *et al.* (1999a, b): young (< 1 year old), mature (*S. tenacissima*: 1 to 1.5 years old; *R. sphaerocarpa*:

1 to 2 years old), and old (*S. tenacissima*: > 1.5 years old; *R. sphaerocarpa*: > 2 years old). The photosynthetic capacity assigned to these three categories of photosynthetic tissues is shown in Table 3. The effects of tissue ageing on potential carbon gain by the whole canopy were explored by running the model with the photosynthetic surfaces arranged in three different ways: (1) all photosynthetic tissues young; (2) 33% of the photosynthetic tissues young, and 66% mature; and (3) 33% of the photosynthetic tissues young, 33% mature, and 33% old. For simulations where tissue age does not enter as a variable, carbon gain was calculated for the plant crown having all its photosynthetic surfaces young and exhibiting the maximal  $A_{\max}$  for a given season of the year.

## RESULTS

The fraction of the total photosynthetic surface area projected to a direction of incident PPFD ( $E_p$ ) varied with solar elevation, but this variation was small and the mean  $E_p$  was rather low for both species compared to a horizontal surface (Fig. 5). The low values of  $E_p$  were essentially caused by the steep angle of the photosynthetic surfaces (Figs 3 and 4). Despite the similar behaviour of  $E_p$  as a function of elevation, significant differences were found between the two species at either very low or very high solar elevations.  $E_p$  in *S. tenacissima* was lower than in *R. sphaerocarpa* for angles over  $65^\circ$ , while the reverse was true for angles below  $15^\circ$ . Both species had 15–20% of their foliage shaded for most elevations, but *S. tenacissima* exhibited a sharp increase in self-shading for elevations over  $75^\circ$  (Fig. 5). The fraction of the photosynthetic surface area displayed ( $E_d$ , i.e. projected minus self-shaded areas) was low in both species (less than 40% for most elevations). However, the fraction of photosynthetic surface area of *S. tenacissima* displayed to the brightest regions of the sky (high solar elevations) was significantly smaller than that of *R. sphaerocarpa*, due to the combination of low  $E_p$  and high self-shading.

Differences in the canopy architecture of the two species resulted in each having very different patterns of daily PPFD interception. Throughout the year, *S. tenacissima* intercepted only about half of the daily PPFD intercepted by *R. sphaerocarpa* under the same conditions (Fig. 6). Both species intercepted less PPFD per day than a horizontal surface, except in winter, when *R. sphaerocarpa* intercepted significantly more due to the low elevation angle of the sun during this season. Species differences were more apparent for the intercepted PPFD above the saturation point (i.e. at which 90% of  $A_{\max}$  was reached). While *R. sphaerocarpa* intercepted 5–9  $\text{mol m}^{-2} \text{d}^{-1}$  PPFD above saturation, *S. tenacissima* intercepted almost no PPFD above saturation (Fig. 6).

The combination of high light interception and high  $A_{\max}$  of *R. sphaerocarpa* resulted in a potential daily carbon gain two–three times larger than in *S. tenacissima* for most of the year (Fig. 6). When the effect of differences due to  $A_{\max}$  were overcome by expressing carbon gain as a percentage of that achieved by a horizontal surface with the same  $A_{\max}$ , differences between the two species became minimal during the summer (40–60% potential daily carbon gain of that of

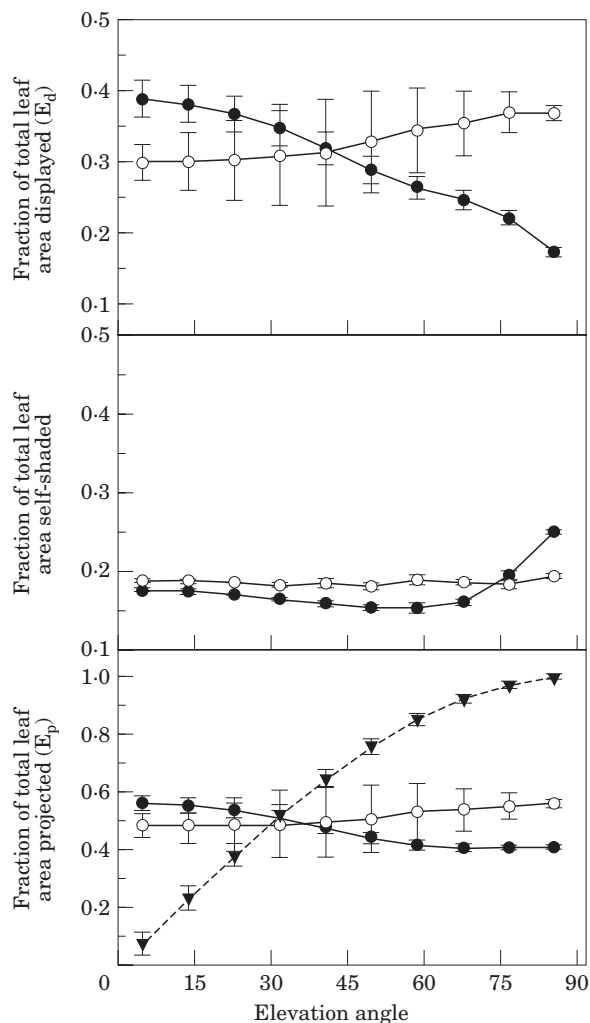


FIG. 5. Projection efficiency (fraction of total leaf area projected,  $E_p$ ), self shading, and display efficiency (fraction of total leaf area displayed,  $E_d$ ) as a function of solar elevation angle for *Stipa tenacissima* (●) and *Retama sphaerocarpa* (○).  $E_p$  is also shown for a horizontal surface (▼). Each point is the mean  $\pm$  s.d. for all azimuths at that elevation. Leaf area in the case of *R. sphaerocarpa* is photosynthetic surface of cladodes.

an equivalent horizontal surface) and largest in winter, when *R. sphaerocarpa* exhibited a potential carbon gain 90% of that of a horizontal surface, while *S. tenacissima* maintained its value around 40% (Fig. 6).

The effect of tissue ageing on potential carbon gain for the whole crown was small for these two species. Simulations with two age-classes of photosynthetic tissues (33% young, 66% mature) reduced potential daily assimilation by only 6%, and simulations with three age classes (33% young, 33% mature, 33% old) reduced potential daily assimilation by 10% (Fig. 7). This contrasts with the large changes in carbon gain at the whole-crown level across the seasons. Summer drought reduced the potential carbon gain in the two species by 55–63% (Fig. 7). The highest photosynthetic activity and consequently the largest potential carbon gain was in spring for *S. tenacissima* and autumn for *R. sphaerocarpa*.

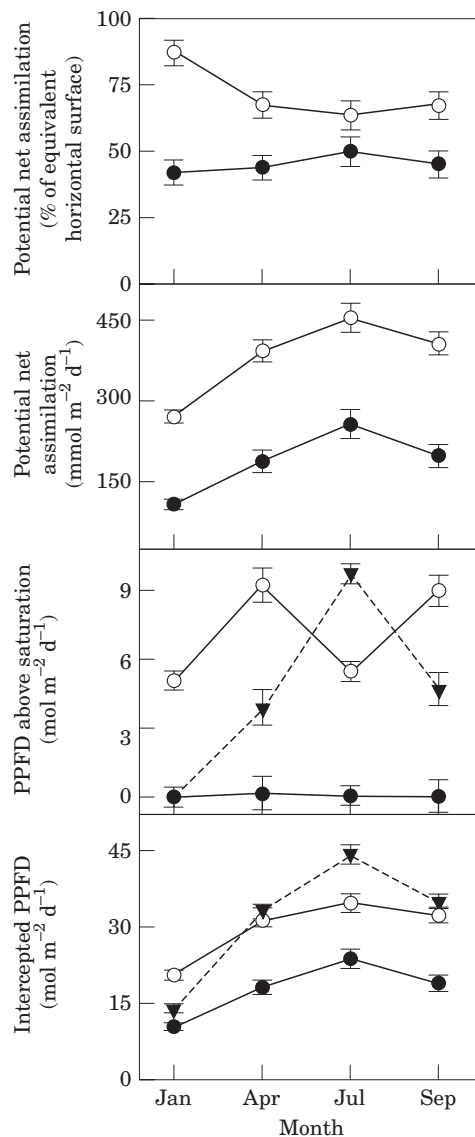


FIG. 6. Total PPFD intercepted per day, intercepted PPFD above the light saturation point for photosynthesis, and potential net assimilation (as daily carbon gain, and as a percentage of an equivalent photosynthetic surface placed horizontally and without self-shading of reconstructed plants of *Stipa tenacissima* (●) and *Retama sphaerocarpa* (○) for the different seasons of the year. Interception of PPFD by a horizontal surface (—▼—) is also provided. Mean of 5 d  $\pm$  s.d.

To better understand the structural factors involved in the avoidance of irradiance exhibited by tussocks of *S. tenacissima*, we explored the functional implications of changes in the amount of photosynthetic and non-photosynthetic leaves. The percentage of total foliage represented by green leaves may vary between 40 and 100% in response to environmental conditions (Haase *et al.*, 1999b). Increasing the photosynthetic surface of the tussocks increased  $E_p$  at the highest elevation angles (Fig. 8), because of a small increase of nearly horizontal portions of the foliage. However, self-shading increased with increasing leaf area. At low to intermediate values of leaf area, the increase in  $E_p$  with leaf area overrode the increase in self-shading, and the

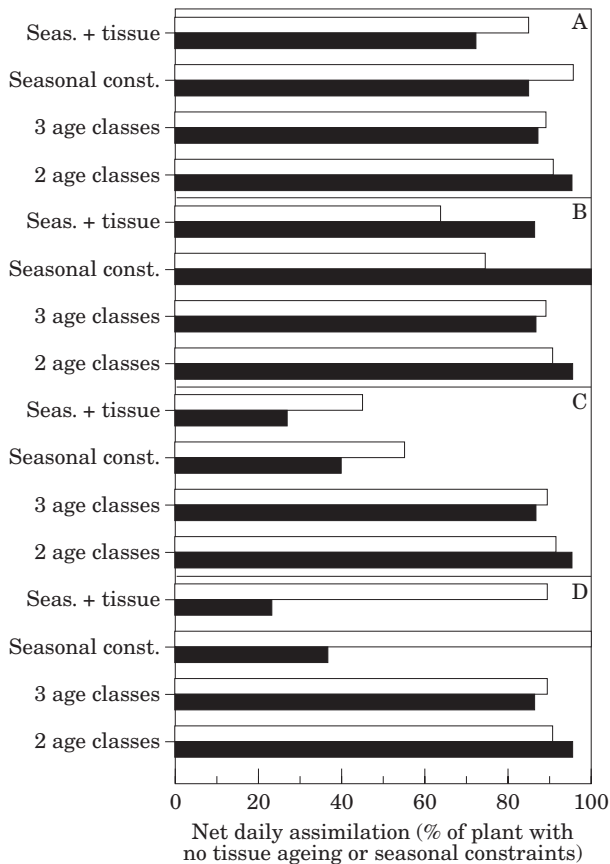


FIG. 7. Influence of tissue ageing and seasonal constraints of photosynthesis on net daily carbon gain of reconstructed plants of *Stipa tenacissima* (■) and *Retama sphaerocarpa* (□) in January (A), April (B), July (C) and September (D). The effects of tissue ageing were simulated considering either two age classes (33% of the photosynthetic surface area young and 66% mature, see Materials and Methods, and Table 3) or three age classes (33% young, 33% mature and 33% old). Values are expressed as percentage of the net carbon gain of the same plant without any tissue ageing or seasonal constraint of photosynthesis. Error bars not given for clarity.

fraction of foliage displayed to the brightest regions of the sky paralleled the increase in leaf area (Fig. 8). But after reaching a given value of leaf area (in this case, around 2000 cm<sup>2</sup>), the self-shading effects became more important than the increasing E<sub>p</sub>, and the fraction of the foliage displayed decreased with increasing leaf area. However, interception of PPF<sub>D</sub> during the central hours of the day and total PPF<sub>D</sub> intercepted throughout the day were little affected by changes in the total leaf area within the range explored (Fig. 8). Potential net assimilation did decrease with increasing leaf area because of changes in the relative contribution of direct and diffuse PPF<sub>D</sub> to total daily PPF<sub>D</sub>.

The contribution to avoidance of excessive irradiance by senesced leaves that remain attached to the tussock was not significant. A change in the senesced leaf area from 0 to 2000 cm<sup>2</sup> (i.e. from 0 to 50% of the total foliage of the tussock) caused almost no change in E<sub>p</sub> and E<sub>d</sub> of the photosynthetically-active leaf area (Fig. 9). PPF<sub>D</sub> interception and potential carbon gain, both at midday and

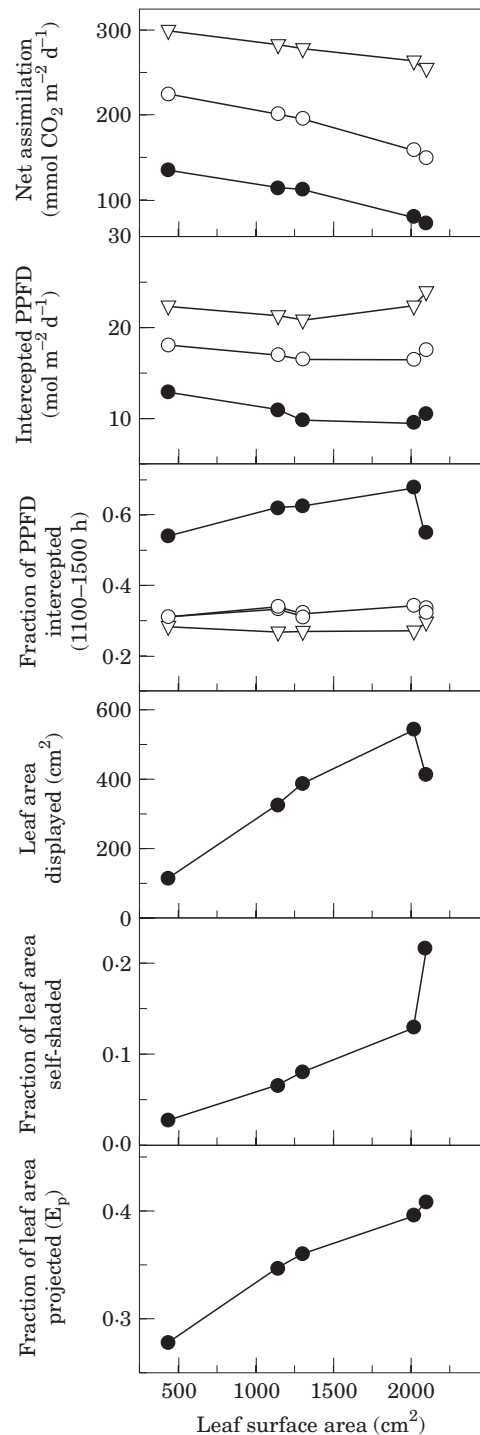


FIG. 8. Fraction of photosynthetically active leaf area projected and self-shaded, and photosynthetically active leaf area displayed to the most luminous regions of the sky (regions of an elevation angle > 45° and falling within the sunpath), and PPF<sub>D</sub> intercepted at midday and during the whole day, and potential net assimilation of reconstructed plants of *Stipa tenacissima* of varying photosynthetically active leaf area. Values of PPF<sub>D</sub> interception and potential carbon gain are given independently for January (●), April and September (○), and July (▽). Error bars are smaller than symbols.

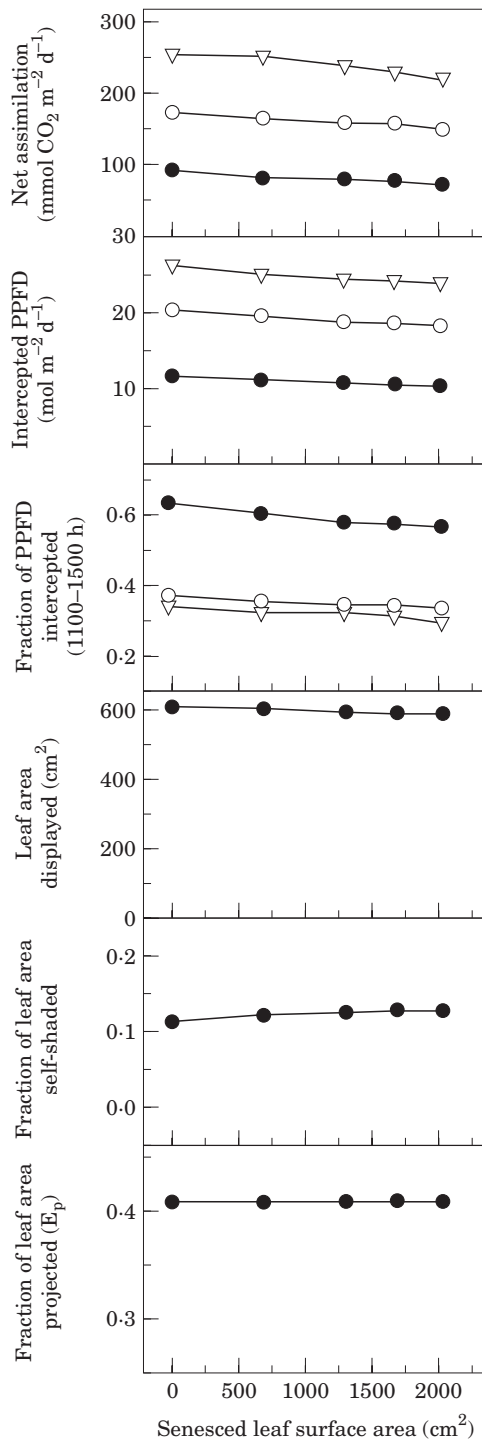


FIG. 9. Fraction of photosynthetically active leaf area projected and self-shaded, and photosynthetically active leaf area displayed to the most luminous regions of the sky (regions of an elevation angle > 45° and falling within the sunpath), and PPFD intercepted at midday and during the whole day, and potential net assimilation of reconstructed plants of *Stipa tenacissima* with varying areas of senesced leaves. Values of PPFD interception and potential carbon gain are given independently for January (●), April and September (○), and July (▽). Error bars are smaller than the symbols.

integrated throughout the day, slightly decreased with increasing senesced leaf area of the tussock throughout the year.

### DISCUSSION

The model simulations indicated that by attenuating radiation loads at midday, especially during the summer, canopy architecture of both *S. tenacissima* and *R. sphaerocarpa* minimized the risk of overheating and photooxidative destruction of the photosynthetic apparatus. Steeply oriented foliage and a moderate self-shading reduced the photosynthetic surface exposed during the central hours of the day to less than 50% of the total leaf area of the canopy. However, the model calculations indicated that this structural photoprotection came at an elevated cost in terms of missed opportunity for carbon fixation in these two species: potential carbon gain (assuming no environmental constraint) of the whole canopy for a given summer day was only 40–60% of that of an equivalent, horizontal photosynthetic surface. The relevance of this cost becomes clearer when compared with the reduction caused by water shortage: summer drought alone (*via* reduced stomatal conductance and mesophyll limitations) decreased potential carbon gain of the whole canopy by 55–63% in both species. The missed opportunity for carbon gain due to structural avoidance of irradiance is very relevant in *R. sphaerocarpa* because its deep root system—with access to deep water stores—and high photosynthetic rates (Haase *et al.*, 1996, 1999a) would allow a significantly higher CO<sub>2</sub> uptake in late spring and most of the summer if the photosynthetic surfaces intercepted more radiation. The structural avoidance of irradiance could have analogous negative implications in the case of *S. tenacissima* because this species responds opportunistically to occasional pulses of water that occur during the summer (Pugnaire *et al.*, 1996a), and a low interception of available light during these events is clearly disadvantageous from the point of view of yield. Irradiance avoidance by the canopy of these two species seemed to be important not only during the summer, but also during the active growth season (spring in the case of *S. tenacissima* and autumn in the case of *R. sphaerocarpa*; see Fig. 6). The elevated cost of structural photoprotection obtained with whole crown model simulations emphasizes the ecological relevance of avoiding high light stress in semi-arid environments. This preventive strategy seems advantageous in environments with unpredictable limiting resources, as is the case for water availability in Mediterranean-type ecosystems (Valladares and Percy, 1997, 1998).

By simulating light interception and carbon gain in two tussock grasses of semi-arid steppe regions of the Rocky Mountains (USA), Ryel *et al.* (1993) observed that neither species appeared to sacrifice carbon gain with steep foliage orientation. However, the species studied differed in the calculated benefits of steep foliage in terms of potential whole-canopy photosynthesis. The differences were accounted for by differences in tussock density: sparse tussocks can achieve higher daily carbon gain with horizontal as opposed to steep foliage, while the reverse is true for dense tussocks. Steep leaf angles also enhanced carbon gain in the

relatively dense chaparral shrub *Heteromeles arbutifolia* by allowing a better distribution of irradiance within the canopy (Valladares and Pearcy, 1998). Leaf area index (LAI) is crucial in determining the influence of crown architecture in general, and leaf angle in particular, on light harvesting and canopy photosynthesis. When LAI is small, as is the case in many plants from arid environments such as those studied here, the geometry of the foliage exerts a large influence on the diurnal and seasonal patterns of light capture and potential carbon gain.

Canopy geometries differed widely in *R. sphaerocarpa* and *S. tenacissima*, and so did light interception. Both species showed steep photosynthetic surfaces, but the open crown of *R. sphaerocarpa* translated into a larger PPFD interception than in the closed tussocks of *S. tenacissima*, where radiation avoidance was enhanced by high self-shading for the brightest regions of the sky and little light penetration within the tussocks. The ability of *S. tenacissima* to almost completely avoid PPFDs above those saturating for photosynthesis (Fig. 6) confirmed our hypothesis that this species could exhibit greater photoprotection than *R. sphaerocarpa*. This hypothesis was based on the seasonality and duration of the growth periods of the two species in the field (see Materials and Methods) determined by the extension of their root system. Since radiation avoidance has a cost in terms of reduced carbon gain, *R. sphaerocarpa*, photosynthetically active throughout the year, reached a more positive balance between light interception for photosynthesis and avoidance of potentially dangerous PPFDs above saturation.

The amount of photosynthetic components in leaves decreases with leaf ageing because proteins are degraded and their breakdown products are translocated to other plant parts (Stoddart and Thomas, 1982; Chapin and Kedrowsky, 1983). Consequently, the rate of light-saturated photosynthesis decreases with leaf age (Reich, Walters and Ellsworth, 1991). As older leaves are generally overtopped by young leaves, two vertical gradients from the upper to the lower parts of the plant occur simultaneously, one of decreasing photosynthetic capacity and the other of decreasing PPFD availability (Hirose *et al.*, 1988; Hikosaka *et al.*, 1993). The contribution to whole plant carbon gain made by old and shaded leaves in lower positions of the canopy has not attracted much attention despite its ecological interest (Caldwell *et al.*, 1986). The simulations performed here with *S. tenacissima* and *R. sphaerocarpa* revealed little impact of tissue ageing on the potential carbon gain of the crown (Fig. 7). Since this impact becomes more significant when PPFD intercepted by the tissue is close to saturation (i.e. when the maximum rate of photosynthesis can be achieved), and both species intercepted least PPFD near or above saturation, the effects of tissue ageing on canopy photosynthesis were minor.

Steep foliage and dense grouping of tillers are characteristics of many tussock grasses from arid environments (Ryel, Beyschlag and Caldwell, 1994; Sánchez and Puigdefábregas, 1994). The benefits in terms of water use efficiency and avoidance of photoinhibition of this growth form have been illustrated using a statistical whole-plant model (Ryel and Beyschlag, 1995). A poorly known aspect

of the tussock growth form in relation to light interception and photosynthesis is the change in foliage display efficiency with increasing photosynthetic surface. Most plants show a decrease in foliage display efficiency with increasing leaf area which translates into decreased light interception, i.e. radiation avoidance increases with leaf area. However, the decrease in the display of photosynthetically active leaf areas in tussocks of *S. tenacissima* was not followed by a parallel decrease in PPFD interception per day due to the opposing effects of increased self-shading and increased projection efficiency (Fig. 8). We concluded that structural avoidance of excess radiation in *S. tenacissima* tussocks with less than 500 cm<sup>2</sup> of green surface is similar to that of tussocks of slightly more than 2000 cm<sup>2</sup> of leaf area. This high radiation avoidance even in small plants of *S. tenacissima* may have important advantages for the establishment of seedlings of this species in open and stressful environments.

Another structural aspect of many tussock grasses of potential relevance for light interception and avoidance is the persistence of senesced leaves. Our results (Fig. 9) show that, for a medium-size tussock of *S. tenacissima*, changes in the amount of senesced foliage from 0 to 50% of the total have only a small impact on PPFD interception and potential carbon gain. It seems that the possible photoprotective role of senesced foliage is very low in comparison with the avoidance of incident PPFD by the dense and steep canopy elements of the tussocks of this species. However, the role of these senesced leaves could be significant in keeping the long leaves of the canopy upright, forming a close tussock.

Plants have several physiological mechanisms to protect photosystem II (PSII) from excess light by dissipating, non-photochemically, part of the excitation energy reaching leaves (Demmig-Adams and Adams, 1992; Chaumont, Morot-Gaudry and Foyer, 1995). This physiological photoprotection is quickly reversible, and the efficiency of light use usually recovers in minutes, unless long-term down-regulation is 'locked-in' or the photosynthetic machinery has been severely damaged (Anderson *et al.*, 1993). However, physiological photoprotection mechanisms are energy-dependent processes with an associated metabolic cost. On the contrary, structural avoidance of radiation is usually irreversible in the short term [with the exception of diurnal movements of leaves in a reduced number of species (Ehleringer and Forseth, 1980; Ludlow and Björkman, 1984)], but has no costs except for the missed opportunity for carbon gain discussed above. In addition, steep structures are mechanically cheaper than horizontal structures in terms of the biomass required to hold them (Niklas, 1992; Givnish, 1995; Valladares, 1999), so canopies such as those studied here require less allocation to supporting structures and have more biomass allocated to photosynthetic structures. The costs in terms of missed opportunity for carbon gain due to photoprotection by dynamic photoinhibition has seldom been estimated (Long *et al.*, 1994). Structural avoidance of radiation by crown architecture consisting of cylindrical, opaque, vertically-oriented photosynthetic surfaces was on the verge of limiting the productivity of cacti even in the high-radiation environments of deserts (Nobel,

1986). More studies are still necessary to assess, realistically, the cost-benefit of these two methods of photoprotection in nature. However, our study, and earlier works on sclerophylls, cacti and tussock grasses (Nobel, 1986; Pugnaire and Haase, 1995; Ryel and Beyschlag, 1995; Valladares and Percy, 1998; Valladares, 1999) suggest that structural photoprotection is a very effective strategy to cope with high irradiance stress in poor and adverse habits such as arid environments.

#### ACKNOWLEDGEMENTS

This study has benefited from expertise and fitting criticisms of Robert W. Percy, David W. Lawlor and three anonymous referees. Thanks are due to Miguel Angel Rubio (Plataforma Solar de Almería) for providing irradiance data. The research was supported by the Spanish CICYT (Grant AMB98-1108-C04-01) and the Ministry for Education and Culture (postdoctoral contract to F.V.).

#### LITERATURE CITED

- Anderson JM, Chow WS, Öquist G. 1993. Dynamics of Photosystem II: photoinhibition as a protective acclimation strategy. In: Yamamoto HY, Smith CM, eds *Photosynthetic responses to the environment*. New York: American Society of Plant Physiologists, 14–26.
- Caldwell MM, Meister HP, Tenhunen JD, Lange OL. 1986. Canopy structure, light microclimate and leaf gas exchange of *Quercus coccifera* L. in a Portuguese macchia: measurements in different canopy layers and simulations with a canopy model. *Trees* 1: 25–41.
- Chapin FS III, Kedrowski RA. 1983. Seasonal changes in nitrogen and phosphorus fractions and autumn retranslocation in evergreen and deciduous taiga trees. *Ecology* 64: 376–391.
- Chaumont M, Morot-Gaudry JF, Foyer CH. 1995. Effects of photoinhibitory treatment on CO<sub>2</sub> assimilation, the quantum yield of CO<sub>2</sub> assimilation, D<sub>1</sub> protein, ascorbate, glutathione and xanthophyll contents and the electron transport rate in vine leaves. *Plant, Cell and Environment* 18: 1358–1366.
- Demmig-Adams B, Adams WW. 1992. Photoprotection and other responses of plants to high light stress. *Annual Review of Plant Physiology and Plant Molecular Biology* 43: 599–626.
- Dickmann DI, Michael DA, Isebrands JG, Westin S. 1990. Effects of leaf display on light interception and apparent photosynthesis in two contrasting *Populus* cultivars during their second growing season. *Tree Physiology* 7: 7–20.
- Ehleringer J, Forseth I. 1980. Solar tracking by plants. *Science* 210: 1094–1098.
- Gamon JA, Percy RW. 1989. Leaf movement, stress avoidance and photosynthesis in *Vitis californica*. *Oecologia* 79: 475–481.
- Gamon JA, Percy RW. 1990. Photoinhibition in *Vitis californica*—interactive effects of sunlight, temperature and water status. *Plant, Cell and Environment* 13: 267–275.
- Givnish TJ. 1995. Plant stems: biomechanical adaptation for energy capture and influence on species distributions. In: Gartner BL, ed. *Plant stems: physiology and functional morphology*. San Diego, California: Academic Press, 3–49.
- Haase P, Pugnaire FI, Fernández EM, Puigdefábregas J, Clark SC, Incoll LD. 1996. Investigation of rooting depth in the semi-arid shrub *Retama sphaerocarpa* (L.) Boiss. by labelling of ground water with a chemical tracer. *Journal of Hydrology* 170: 23–31.
- Haase P, Pugnaire FI, Clark SC, Incoll LD. 1999a. Canopy dynamics and photosynthetic rate in three perennial species in semi-arid south-eastern Spain. Stem photosynthesis in the shrub *Retama sphaerocarpa*. *Functional Ecology* (in press).
- Haase P, Pugnaire FI, Clark SC, Incoll LD. 1999b. Dynamics of leaf area and photosynthetic rate of the tussock grass *Stipa tenacissima* in semi-arid south-eastern Spain. *Functional Ecology* (in press).
- Herbert T. 1996. On the relationship of plant geometry to photosynthetic response. In: Mulkey SS, Chazdon RL, Smith AP, eds. *Tropical forest plant ecophysiology*. New York: Chapman and Hall, 139–161.
- Hikosaka K, Okada K, Terashima I, Katoh S. 1993. Acclimation and senescence of leaves: their roles in canopy photosynthesis. In: Yamamoto HY, Smith CM, eds. *Photosynthetic responses to the environment*. New York: American Society of Plant Physiologists, 1–13.
- Hirose T, Werger M, Pons T, van Rheeën J. 1988. Canopy structures and leaf nitrogen distribution in a stand of *Lysimachia vulgaris* L. as influenced by a stand density. *Oecologia* 77: 145–150.
- Horton P, Ruban AV, Walters RG. 1996. Regulation of light harvesting in green plants. *Annual Review of Plant Physiology and Plant Molecular Biology* 47: 655–684.
- Larcher W. 1995. *Physiological plant ecology. Ecophysiology and stress physiology of functional groups*. 3rd edn. Berlin-Heidelberg: Springer-Verlag.
- Long SP, Humphries S, Falkowski PG. 1994. Photoinhibition of photosynthesis in nature. *Annual Review of Plant Physiology and Plant Molecular Biology* 45: 633–662.
- Ludlow MM, Björkman O. 1984. Paraheliotropic leaf movement in *Siratro* as a protective mechanism against drought-induced damage to primary photosynthetic reactions: damage by excessive light and heat. *Planta* 161: 505–518.
- McMillen GG, McClendon JH. 1979. Leaf angle: an adaptive feature of sun and shade leaves. *Botanical Gazette* 140: 437–442.
- Niklas KJ. 1988. The role of phyllotactic pattern as a 'developmental constraint' on the interception of light by leaf surfaces. *Evolution* 42: 1–16.
- Niklas KJ. 1992. *Plant biomechanics: an engineering approach to plant form and function*. Chicago: Chicago University Press.
- Nobel PS. 1986. Form and orientation in relation to PAR interception by cacti and agaves. In: Givnish TJ, ed. *On the economy of plant form and function*. New York: Cambridge University Press, 83–104.
- Percy RW, Yang W. 1996. A three-dimensional shoot architecture model for assessment of light capture and carbon gain by understory plants. *Oecologia* 108: 1–12.
- Percy RW, Yang W. 1998. The functional morphology of light capture and carbon gain in the redwood-forest understory plant, *Adenocaulon bicolor* Hook. *Functional Ecology* 12: 543–552.
- Powles SB. 1984. Photoinhibition of photosynthesis induced by visible light. *Annual Review of Plant Physiology and Plant Molecular Biology* 35: 15–44.
- Pugnaire FI, Haase P. 1995. Comparative physiology and growth of two perennial tussock grass species in a semi-arid environment. *Annals of Botany* 77: 81–86.
- Pugnaire FI, Haase P, Incoll LD, Clark SC. 1996a. Response of the tussock grass *Stipa tenacissima* to watering in a semi-arid environment. *Functional Ecology* 10: 265–274.
- Pugnaire FI, Haase P, Puigdefábregas J. 1996b. Facilitation between higher plant species in a semiarid environment. *Ecology* 77: 1420–1426.
- Reich PB, Walters MB, Ellsworth DS. 1991. Leaf age and season influence the relationships between leaf nitrogen, leaf mass per area and photosynthesis in maple and oak trees. *Plant, Cell and Environment* 14: 251–259.
- Ryel RJ, Beyschlag W. 1995. Benefits associated with steep foliage orientation in two tussock grasses of the American Intermountain West. A look at water-use-efficiency and photoinhibition. *Flora* 190: 251–260.
- Ryel RJ, Beyschlag W, Caldwell MM. 1993. Foliage orientation and carbon gain in two tussock grasses are assessed with a new whole-plant gas-exchange model. *Functional Ecology* 7: 115–124.
- Ryel RJ, Beyschlag W, Caldwell MM. 1994. Light field heterogeneity among tussock grasses: theoretical considerations of light harvesting and seedling establishment in tussocks and uniform tiller distributions. *Oecologia* 98: 241–246.
- Sánchez G. 1995. *Dinámica y transformaciones espaciales de las matus de esparto (Stipa tenacissima L.) y su interacción con el transporte de sedimentos*. PhD Thesis, Universidad Autónoma de Madrid, Spain.

- Sánchez G, Puigdefábregas J. 1994.** Interactions of plant growth and sediment movement on slopes in a semi-arid environment. *Geomorphology* **9**: 243–260.
- Smith M, Ullberg D. 1989.** Effect of leaf angle and orientation on photosynthesis and water relations in *Silphium terebinthinaceum*. *American Journal of Botany* **76**: 1714–1719.
- Stoddart JL, Thomas H. 1982.** Leaf senescence. In: Boulter D, Pathier B, eds. *Encyclopedia of plant physiology. Vol 14A*. Berlin: Springer-Verlag.
- Takenaka A. 1994.** A simulation model of tree architecture development based on growth response to local light environment. *Journal of Plant Research* **107**: 321–330.
- Valladares F. 1999.** Architecture, ecology and evolution of plant crowns. In: Pugnaire FI, Valladares F, eds. *Handbook of functional plant ecology*. New York: Marcel Dekker, 121–194.
- Valladares F, Pearcy RW. 1997.** Interactions between water stress, sun-shade acclimation, heat tolerance and photoinhibition in the sclerophyll *Heteromeles arbutifolia*. *Plant, Cell and Environment* **20**: 25–36.
- Valladares F, Pearcy RW. 1998.** The functional ecology of shoot architecture in sun and shade plants of *Heteromeles arbutifolia* M. Roem., a Californian chaparral shrub. *Oecologia* **114**: 1–10.
- Werk KS, Ehleringer J. 1984.** Non-random leaf orientation in *Lactuca serriola* L. *Plant, Cell and Environment* **7**: 81–87.